X-ray and UV-Vis-NIR absorption spectroscopy studies of the Cu(I) and Cu(II) coordination environments in mixed alkali-lime-silicate glasses

Lina Grund Bäck[a,b,*], Sharafat Ali[a], Stefan Karlsson[b,c,*], Lothar Wondraczek[c,d], Bo Jonson[a]

[a] Department of Built Environment and Energy Technology, Linnaeus University, SE-35195 Växjö, Sweden
[b] RISE Research Institutes of Sweden, Division of the Built Environment, Glass Section, SE-35196 Växjö, Sweden
[c] Otto Schott Institute of Materials Research, Friedrich Schiller University of Jena Fraunhoferstraße 6, D-07743 Jena, Germany
[d] Abbe Center of Photonics, Friedrich Schiller University of Jena, Max-Wien-Platz 1, D-07743 Jena, Germany

ARTICLE INFO

ABSTRACT

The local structures of Cu(I) and Cu(II) in $(20-x)Na_2O-xK_2O-10CaO-70SiO_2$ glasses with a copper content of 0.4 mol% have been investigated by Cu K-edge extended X-ray absorption fine structure (EXAFS) and X-ray absorption near edge structure (XANES). Complementary data for Cu(II) was derived using UV–Vis-NIR spectroscopy. Indication for mainly linear two-fold coordination of the Cu^+ ion was found by both EXAFS and XANES, but other coordination between Cu^+ and O^{2-} cannot be excluded. The Cu(I)−O bond lengths were found to be 1.79–1.83 ± 0.02 Å. EXAFS results showed that Cu(II) was mostly present in a Jahn-Teller distorted environment with oxygen, an octahedron with four shorter Cu(II)−O bonds and two longer in axial position. The equatorial bond lengths were found to be 1.89–1.91 ± 0.02 Å and the axial 2.20–2.24 ± 0.02 Å with no effect of the Jahn-Teller distortion of the octahedron when the glass composition was altered.

1. Introduction

As CuO is added to the glass melt, the redox equilibria between the cuprous Cu^+ and cupric Cu^{2+} are dependent on the glass composition. It is known that the proportion of Cu^+ will increase if the basicity of the silicate glass increases [1]. Cu^{2+} absorbs light of the longer wavelengths in the visible to near-infrared (NIR) spectral region, resulting in the characteristic turquoise–blue coloration of copper-doped silicate glasses. Cu^+ ions, on the other hand, have a d^{10} electronic configuration and thus no empty d-orbitals; therefore, they are colorless. Both ions are incorporated into the glass structure in different ways and can, in principle, act as glass modifiers or network formers [2]. Due to the presence of assessable *d-d-* transitions in the d^9 Cu^{2+} ion, optical as well as paramagnetic resonance spectroscopy can be used for probing this species' structural environment. For the diamagnetic Cu^+ ion, these techniques are not as readily applicable. Several studies have been published on the structural features of Cu^{2+} in oxide glasses using UV–Vis-NIR spectroscopy and/or EPR (electron paramagnetic resonance spectroscopy) as primary techniques [3–9]. The expected coordination environment for Cu^{2+} from these studies is a Jahn-Teller distorted octahedron with two elongated bonds along the z-axis. However, the degree of distortion and its dependence on glass structure are still unclear, and published interpretations are sometimes contradictory.

EXAFS (Extended X-ray Absorption Fine Structure) studies of the coordination environment of Cu^+ and Cu^{2+} ions have to some extent been made for ion exchanged and ion-implanted glasses [10–15]. Copper oxide was incorporated in the glass matrix during the melting process in aluminosilicate glasses with a CuO concentration of about 20 wt% [16]. It was concluded that the Cu^+ ion was coordinated by two oxygen ions (linear complex), whereas the Cu^{2+} ion was coordinated by four oxygen ions in a square planar geometry. This was confirmed in similar studies of blue Paleo-Christian glass mosaics [17]. There are also examples on green copper glasses, where the $Cu^{2+}–O^{2-}$ coordination geometry is square planar [18]. Thus, there is some discrepancy between interpretations using EPR and UV–Vis-NIR data, and the ones relying on EXAFS. Therefore, in order to further clarify the coordination environment of Cu^{2+} and to sort out the previously contradictory results about the degree of distortion in different silicate glass compositions further studies are needed.

We now investigate the coordination states of Cu^{2+} and Cu^+ as well as the degree of distortion in the Cu^{2+} environment in mixed alkali-lime silicate glasses. This glass system is representative for a broad range of consumer glasses in which copper is used as a coloring agent. Typically, these glasses used further finding agents, which, in turn, affect the redox states of the copper species. Five glasses with the base

Table 1
Nominal glass compositions in mol%.

Sample code	SiO$_2$	Na$_2$O	K$_2$O	CaO	CuO	Sb$_2$O$_3$	CeO$_2$
0 K	69.94	19.66	–	9.98	0.4	–	–
5 K	69.74	14.90	4.99	9.95	0.4	–	–
10 K	69.72	9.95	9.95	9.95	0.4	–	–
15 K	69.71	4.98	14.93	9.95	0.4	–	–
20 K	69.71	–	19.91	9.98	0.4	–	–
0 KSb	69.93	19.90	–	9.95	0.2	0.30	–
20 KSb	69.92	–	19.91	9.95	0.2	0.30	
0 KCe	69.42	19.84	–	9.92	0.2	–	0.60

glass composition of 70SiO$_2$-20R$_2$O-10CaO (R = Na, K) doped with 0.4 mol% CuO have been investigated by means of UV–Vis-NIR spectroscopy and X-ray Absorption Spectroscopy. Furthermore, another two glasses with the same base glass composition containing 0.2 mol% CuO are studied. In one glass 0.3 mol% Sb$_2$O$_3$ were added as a reduction agent in order to shift the redox equilibrium to Cu$^+$, while additions of 0.6 mol% CeO$_2$ were used to favor the oxidation of Cu$^+$ ions to Cu^{2+}.

2. Experimental procedure

2.1. Sample preparation

The glass compositions studied have the nominal molar composition 20R$_2$O-10CaO-70SiO$_2$ (R = Na and/or K). 0.4 mol% of CuO was added to the batch. The glass compositions are listed in Table 1. The raw materials were of industrial grade with maximum 0.01 wt% Fe$_2$O$_3$ and 0.04 wt% Al$_2$O$_3$, using carbonates for the alkali and the alkaline earth components All samples were melted in Pt-Rh crucibles at 1420 °C in batches corresponding to 150 g of glass. Samples were melted in a standard procedure described elsewhere [6,19].

2.2. UV-Vis-NIR spectroscopy

Samples were prepared by grinding and polishing to plane parallel specimens with a thickness of 3–5 mm. All samples were made in doubles or triplets.

A double-beam spectrophotometer (Agilent Technologies, Cary 5000) was used for the measurements. The scan rate was 600 nm/min with a slit width of 2 nm. For the analysis, the samples were masked with a circular aperture with the diameter of 5 mm and were measured from 3300 nm to 200 nm with spectral resolution of 1 nm. The observed absorption band was deconvoluted by using the software Peak Fit® [20].

2.3. X-ray absorption spectroscopy – data collection

Glass samples for the measurements were prepared by crushing and sieving to a particle size below 45 μm, using a 325-mesh sieve. The crystalline reference samples of Cu$_2$O and CuO were treated with mortar and pester and were mixed thoroughly with boron nitride in order to achieve homogenous samples with approximately the same concentration of copper as in the glassy samples. Pure crystalline Cu$_2$O and CuO for reference were also prepared by spreading on a plastic tape.

Copper K-edge X-ray absorption measurements were performed at the wiggler beamline I811 at the Max–II ring [21], Max-lab, Lund, Sweden, during two individual campaigns. The Max-II synchrotron ring offered electron beam energies of 1.5GeV, maximum current of 200 mA and X-rays in the energy range 2.4–20 keV. The beamline was equipped with a Si [111] double crystal monochromator. In order to remove higher harmonics, 30% detuning was used. The sample spectra were collected in fluorescence mode by a solid-state PIPS detector and a metallic Cu reference foil for energy calibration was simultaneously

measured in transmission mode. The measurements were performed at ambient room temperature. The energy scales of the x-ray absorption spectra were calibrated by assigning the first inflection points of the K edges of foils of copper at 8980.3 eV. The ion chambers I$_0$, I$_1$ and I$_2$ were filled with 1.1 bar N$_2$, 0.1 bar Ar and 2 bar Ar respectively. Every sample was scanned at least five times in continuous scanning mode.

2.4. X-ray absorption spectroscopy – data analysis

The data analysis was carried out with the program package EXAFSPAK [22]. The pre-edge subtraction and spline removal were performed in a standard procedure. The software FEFF7 [23] was used for modelling the EXAFS region. The XANES region was only analyzed qualitatively.

2.5. Structural modelling in FEFF7

When using EXAFSPAK and FEFF7 you need to have an idea how the specific ion is coordinated to get a result. When ions are in amorphous materials, like glass it means that you need a structure of Cu(I) and Cu(II) with oxygen in this case, even if the truth is that the ions are more unorganized than the model suggests. This is important to understand when you read this paper.

Below is the modelling described for Cu$^+$ and Cu^{2+} ions.

Cu(I)

In previous investigations, when Cu$^+$ was introduced in the glass by adding to the batch or by ion exchange, a two-fold coordination state was suggested [10–14,16]. Other authors have proposed a situation where six oxygen ions surround the Cu$^+$ ion in a compressed octahedral site [24]. Both models were tried in the fitting process. The Cu–O distance in crystalline Cu$_2$O was determined by Troger et al. to be 1.85 Å [25]; in the previously mentioned EXAFS studies of Cu$_2$O containing glasses, a range of 1.83–1.85 Å was found [10–16,18]. Based on these values, we chose 1.85 Å for the Cu(I)–O as a starting value for structural optimization. However, both longer and shorter bonds were tried in the fitting process.

Cu(II)

Previous studies of the structural coordination of Cu^{2+} in different glass compositions by UV–Vis spectroscopy and EPR have proposed a coordination environment consisting of an elongated octahedron [3–6,26–31]. On the other hand, EXAFS analysis carried out on ordinary melt-quenched glass, ion-exchanged glass and also historic blue glasses have suggested a square planar coordination with four oxygen ions surrounding the Cu^{2+} ion [14,16,17]. Yet again, EXAFS data from sol-gel derived silicate glasses [32] and also from phosphate glasses [33] have given evidence for the elongated octahedron. Therefore, we once more used both structural models in FEFF7, i.e., the square planar and the elongated octahedron. For a starting value of the Cu(II)–O distance, we used 1.95 Å for the four equatorial bonds, and 2.30 for the Cu(II)–O axial bond. These values were chosen in reference to crystalline CuO (1.95 Å) [25] and previous EXAFS results on Cu^{2+} in silica gel [32] and Cu^{2+} in aqueous solution [34]. The sample containing CeO$_2$ was the first sample to be tested as this was the sample with supposedly the highest proportion of Cu^{2+}; we anticipated it to be the easiest sample for probing the applicability of either of the two Cu^{2+} coordination models.

All previous suggestions of the structure of Cu$^+$ and Cu^{2+} with surrounding O^{2-} in glass were considered during the fitting process for the primary coordination environment. Silicon was chosen as backscatterer for the second coordination shell. It is possible that sodium, potassium and calcium also could be backscatterer, but the model became too complex to involve these ions. Multiple scattering paths were fitted, but the contribution to the fit was very small. Different redox ratios of Cu$^+$ and Cu^{2+} were used during the fitting procedure with starting values taken from ref. [6] where the samples were analyzed by means of a wet chemical method. The coordination number, CN was

Table 2

Fitted EXAFS parameters; coordination number (CN), interatomic distance (R), EXAFS Debye-Waller factor (σ^2), goodness of fit parameter (F-factor), degree of octahedral distortion ($Cu-O_{eq}/Cu-O_{ax}$), (Cu^{2+}/Cu_{tot})-ratio. The range of within the data has been fitted k = 3-12 $Å^{-1}$, except for 0 K k = 3–11 $Å^{-1}$).

Sample code		CN	R (Å)	σ^2 ($Å^2$)	F-factor[a] (%)	$CuO_{eq}/Cu-O_{ax}$	Cu^{2+}/Cu_{tot}	Cu^{2+}/Cu_{tot} ref. [6]
Models with Cu^+ in linear coordination with O^{2-} and Cu^{2+} in a Jahn Teller distorted octahedron.								
0 K	Cu^+–O	**1.3**	1.82	0.0042				
	Cu^{2+}-O_{eq}	**1.3**	1.89	0.0048				
	Cu^{2+}-O_{ax}	**0.7**	2.24	0.0098				
	Cu–Si	1.3	2.82	0.0187				
	Cu–Si	1.3	3.03	0.0102				
		3.3			22	0.84	0.325	0.336
5 K	Cu^+–O	**1.4**	1.83	0.0044				
	Cu^{2+}-O_{eq}	**1.2**	1.90	0.0046				
	Cu^{2+}-O_{ax}	**0.7**	2.20	0.0125				
	Cu–Si	1.4	2.81	0.0260				
	Cu–Si	1.2	3.03	0.0112				
		3.3			28	0.86	0.325	0.320
10 K	Cu^+–O	**1.2**	1.79	0.0017				
	Cu^{2+}-O_{eq}	**1.3**	1.90	0.0006				
	Cu^{2+}-O_{ax}	**0.6**	2.21	0.0169				
	Cu–Si	1.2	2.80	0.0215				
	Cu–Si	1.3	3.01	0.0115				
		3.1			29	0.86	0.275	0.308
15 K	Cu^+–O	**1.3**	1.81	0.0033	37	0.86	0.400	0.305
	Cu^{2+}-O_{eq}	**1.5**	1.91	0.0035				
	Cu^{2+}-O_{ax}	**0.8**	2.22	0.0128				
	Cu–Si	1.3	2.85	0.0224				
	Cu–Si	1.5	3.06	0.0121				
		3.6			37	0.86	0.400	0.305
20 K	Cu^+–O	**1.3**	1.81	0.0042				
	Cu^{2+}-O_{eq}	**1.3**	1.89	0.0029				
	Cu^{2+}-O_{ax}	**0.7**	2.23	0.0109				
	Cu–Si	1.4	2.80	0.0150				
	Cu–Si	1.4	3.02	0.0062				
		3.3			35	0.85	0.325	0.301
0 KCe	Cu^{2+}-O_{eq}	**2.3**	1.93	0.00613				
	Cu^{2+}-O_{ax}	**1.1**	2.18	0.0084				
	Cu^+–O	**1.2**	1.84	0.0045				
	Cu–Si	2.2	3.03	0.0159				
	Cu–Si	1.2	2.74	0.0176				
		4.6				0.89	0.65	0.546[b]
20 KSb	Cu^+–O	**2.2**	1.84	0.00395				
	Cu–Si	1.9	2.92					
	Cu–Si	0.3	3.01					
		2.2					0	0.073[b]
Exp. uncertainty		± 15%	± 0.02	± 20%		± 0.015		

Bold values show contributing bonds to get total CN.

[a] Goodness of fit parameter; the sum of the squares of the differences between experimental and calculated values.

[b] Taken from UV–Vis-measurements and the extinction coefficient from ref [6].

used to express the redox ratio parts of Cu^+ and Cu^{2+}, respectively, in the glass samples. For example, the CN in Table 2 is total if you add the CN for every type of Cu-ion, for example 1.3 + 1.3 + 0.7 = 3.3 for sample code 0 K. And then you can solve the following equation system: 3.3 = 2× + (1-x)6 gives x = 0.675 which is the part of Cu^+. This gives 1–0,675 = 0.325 which will be Cu^{2+}/Cu_{tot}.

3. Results

3.1. Cu K-edge EXAFS

The model with Cu^+ in linear coordination with oxygen and Cu^{2+} surrounded with six oxygen ions in an elongated octahedron was found to be the best model (lowest F-factor). The results from the fitted model are summarized in Table 2. The Fourier transforms of the k^3 weighted EXAFS spectra and the corresponding fits are displayed in Fig. 1.

The shortest Cu−O distance (1.81–1.83 Å) originates from the Cu(I)−O bond. The EXAFS Debye-Waller factor σ [2], which is the variation in bond lengths, was found to be 0.0017–0.0044 $Å^2$.

The Cu(II)−O bond distances are ranging from 1.89 Å to 1.91 Å for

the equatorial (x-y) Cu(II) - O binding, the axial (z) Cu(II)−O bonds have distances ranging from 2.20 to 2.24 Å, see Fig. 2. EXAFS Debye-Waller factor, σ^2, ranging from 0.0006 to 0.0048 $Å^2$ for the equatorial bond lengths, but for the axial Cu(II)−O distance it is higher (0.0098–0.0169 $Å^2$). This means that the bond length distribution for this axial Cu(II)−O is higher than for the shorter bonds.

The distances from the Cu^+ ion and Cu^{2+} ion to silicon was found to be 2.80–2.85 Å and 3.01–3.06 Å, respectively, for the different glass compositions.

3.2. Cu K-edge XANES

Spectra from the XANES region are shown in Fig. 3. The characteristic pre-edge peak at about 8985 eV (which is seen in the crystalline Cu_2O sample) is from the 1 s-$4p_{x,y}$ transition and is attributed to a linear coordination [33]. In the spectra of the glassy samples the same band is present. The peak is more intense as the Cu^+ concentration increases, the ($[Cu^+]/[Cu_{tot}]$) ratio is about 85–90% in the 0 KSb and 20 KSb samples, and about 50% in the 0 KCe sample. It confirms the EXAFS results, suggesting a linear coordination of Cu^+ and two O^{2-}.
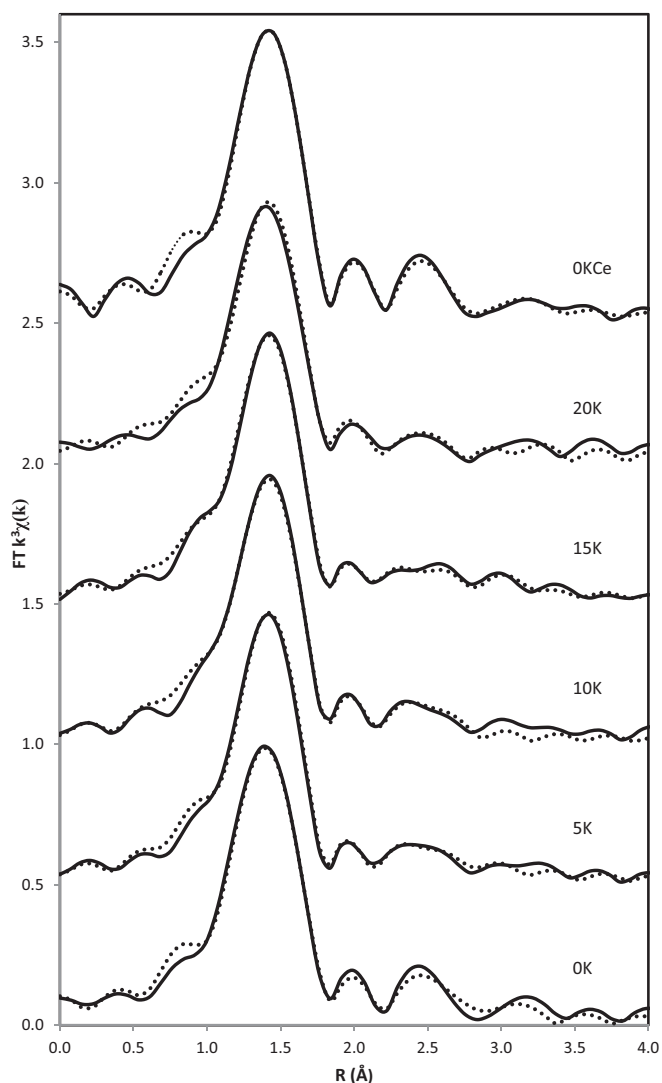
Fig. 1. Fourier transforms of k3-weighted EXAFS spectra (solid lines) and fits (dotted lines). Not corrected for phase shift. 20 K = $70SiO_2$-$10CaO$-$20 K_2O$, 0 K = $70SiO_2$-$10CaO$-$20Na_2O$.

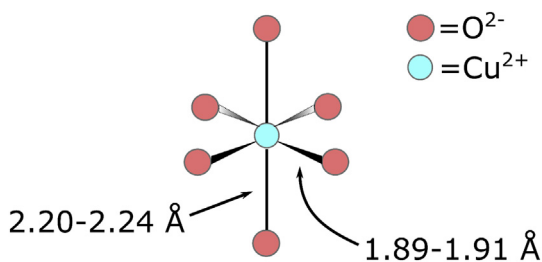**Fig. 2.** Elongated octahedral distorted $[Cu^{2+}(O^{2-})_6]^{-10}$ complex.

There are no obvious transitions in the XANES spectra concerning Cu^{2+}, hence, it cannot be concluded that there is Cu^{2+} other than the indication of less pronounced 1 s-$4p_{x,y}$ transition for Cu^+. However, if the Cu-site has no center of symmetry, there will be a 1 s-3d transition at about 8979 eV [35]. There is no such peak in the studied glass samples, thus the Cu^{2+} coordination environment is probably centrosymmetric.
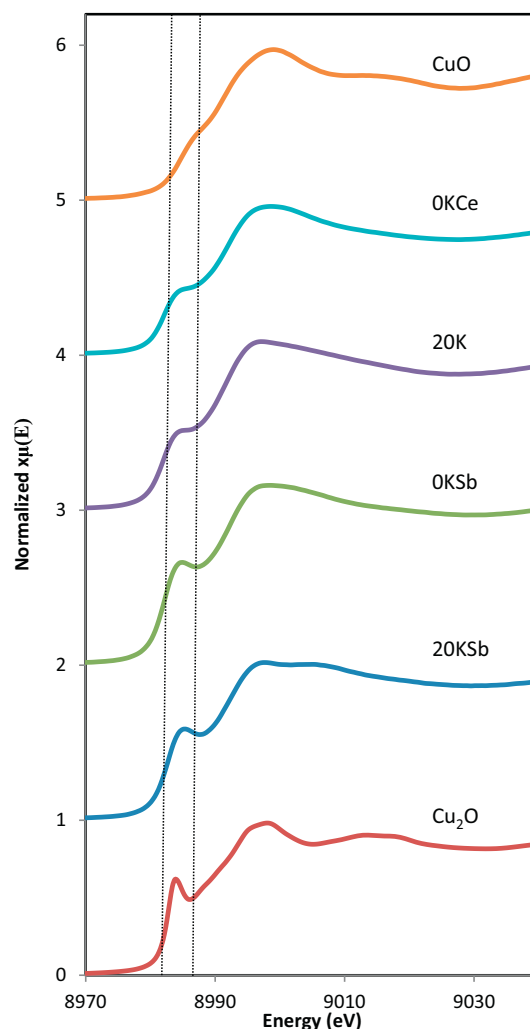

Fig. 3. XANES spectra of selected samples. The dotted lines mark the pre edge peak for the transition 1 s - $4p_{x,y}$ in Cu(I) complex with linear coordination.

3.3. UV–Vis-NIR Spectroscopy

The geometry of an elongated octahedron was expected to give rise to three absorption bands in the UV–Vis-NIR spectra originating from the electronic transitions; dxz, dyz → dx²-y [2], dxy → dx²-y² and dz² → dx²-y [2]. In all spectra, three Gaussian functions were therefore used to decovolute the broad absorption envelope. Results from the deconvolution of the optical absorption spectra are provided in Fig. 4 and Table 3.

3.4. Jahn-Teller distortion of the octahedral complex

The degree of Jahn-Teller distortion of the octahedral complex can be expressed as the ratio between the shorter equatorial bond length and the longer bond length of the complex, Cu-O_{eq}/Cu-O_{ax} [36]. The EXAFS results give us these bond lengths (Table 2). When the ratio is unity there is no distortion at all [36]. The Cu-O_{eq}/Cu-O_{ax} ratio was found to vary only to a small extent, i.e., between 0.84 and 0.86; it is obviously not changing much as the glass composition is varied.

Another way to determine the degree of the Jahn-Teller distortion is to compare the energy needed for the dz² → dx²-y² and dxy → dx²-y² electronic transitions [3]. If the distortion increases (when the axial bond lengths increase) the energy level of the dz² orbital will decrease due to longer distance to the oxygen ligands. The energy levels of dx²-y² and dxy will both increase, but the difference between them will still be
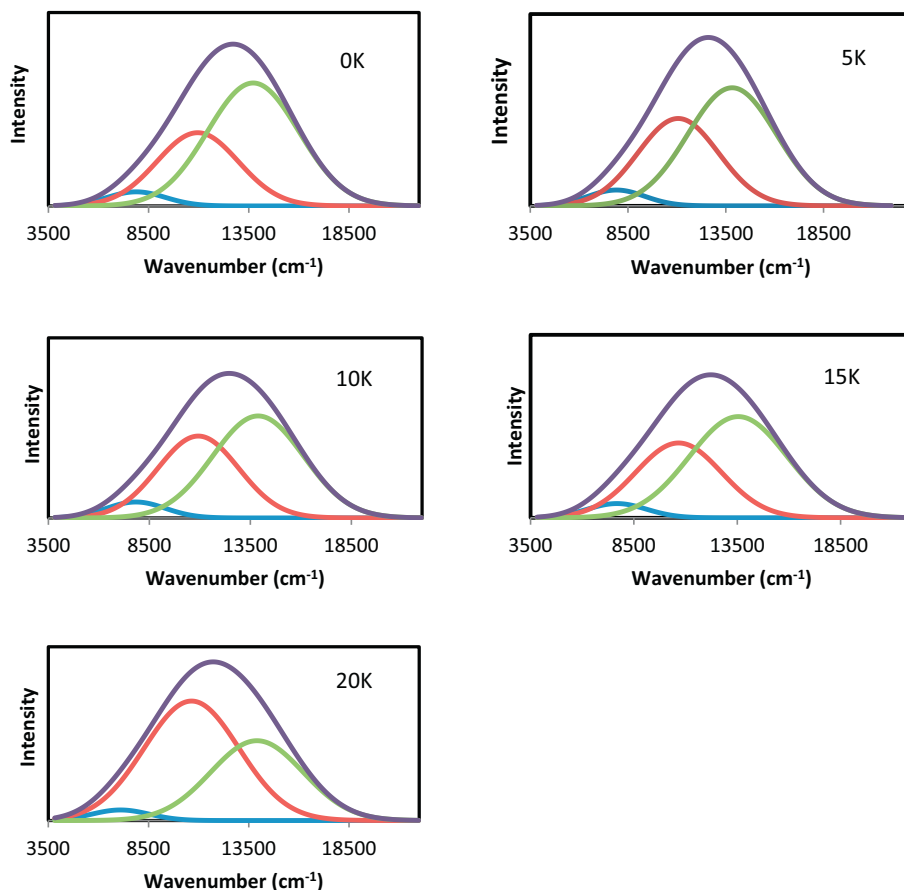
Fig. 4. Deconvoluted UV–Vis-NIR spectra for the different glass compositions.

Table 3
Deconvoluted absorption spectra and octahedral distortion.

Sample code	dxz, dyz →dx²-y² (cm⁻¹)	dxy → dx²-y² (cm⁻¹)	dz² → dx²-y² (cm⁻¹)	T = (dz² → dx²-y²]) / (dxy → dx²-y²])
0 K	13,710	10,950	7880	0.72
5 K	13,830	11,070	7910	0.71
10 K	13,810	10,900	7750	0.71
15 K	13,550	10,660	7680	0.72
20 K	13,300	10,200	7030	0.69
Experimental uncertainty	± 100	± 100	± 100	± 0.02

the same, i.e., the orbital energy increase is constant. The ratio between the transitions $dz^2 \rightarrow dx^2$-y^2 and $dxy \rightarrow dx^2$-y^2 is a measure of the degree of Jahn-Teller distortion (T); the values are found in the range 0.72 to 0.74 for all samples except for the 20 K sample which has ∼ 0.69. The results are summarized in Table 3 through the absorption wavenumbers from UV–Vis-NIR spectroscopy. In this way of representation, the ratio is 0 when there is a regular octahedral. The reason as to why the deconvoluted absorption band for the 20 K glass looks so different from the other glass compositions is presently not clear. It could be related to variations in sample homogeneity, residual thermal stress, local structural compaction or the absence of a mixing effect.

4. Discussion

4.1. Cu(I)—O bond length

The Cu(I)—O distance found in this investigation is somewhat shorter than previous investigations of Cu in glass [10–14,16,17]. Some of the previous studies chose the distance to be constrained to the same distance as found for crystalline Cu_2O (1.847 Å) by X-ray diffraction [25]. On the other hand, when calculating the Cu—O bond length by adding the ionic radii (according to Shannon [37]) of Cu^+ (0.46 Å) and O^{2-} (1.35 Å), the expected Cu—O bond length is 1.81 Å, which is almost identical to our result. As mentioned, it is not likely that all Cu^+ ions are coordinated in a linear way with O^{2-} in an amorphous material as glass. However, we tried out different angles between the Cu^+ and O^{2-} ion and the linear coordination gave the best fit.

4.2. Cu(II)–O bond length

The Cu(II)—O distance found in the present study is shorter compared to most previous studies [14,16,17], but almost the same as found by D'Acapito et al. [11]; the reported a Cu(II)—O distance of 1.92 Å in soda-lime glass implanted with Cu ions.

In two crystalline silicates, $MCuSi_4O_{10}$ (M = Ca and Ba), with Cu(II) coordinated to four oxygen ions in square planar arrangement, the Cu(II)—O distances are 1.928 Å and 1.921 Å, respectively [38]. Thus, in silicates, Cu(II)—O distances are shorter than in, e. g., crystalline CuO (1.95 Å [25]). In water Cu^{2+} is surrounded by six or five ligands and the Cu-O_{eq} were measured to 1.96 and Cu-O_{ax} to 2.29 Å with EXAFS [34,39]. However, in an aerogel silicate the Cu(II)-O_{eq} distance was found to be 1.96–2.00 Å and the Cu(II)-O_{ax} 2.25–2.35 Å by Kristiansen et al. [32]. The axial bond lengths found in the present study are

between 2.20 and 2.24 Å, which is somewhat shorter than the Cu(II) - O^{2-} distance in aerogel or the hexa-aqua Cu(II) complex. The Cu(II)–O bond length expected from Shannon's ionic radii [37] of Cu^{2+} (0.73 Å) and O^{2-} (1.40 Å) is approximately 2.13 Å. However, this bond length would be found in a symmetrical octahedron only. When the co-ordination environment is distorted towards an elongated octahedron, the axial bond lengths will be longer and the equatorial bond lengths shorter.

4.3. Distortion of the $[Cu^{2+} O_6^{2-}]^{10-}$ octahedral coordination environment

It has been proposed from UV–Vis-NIR and EPR studies that the degree of distortion is altered when for example Na^+ is replaced by the larger K^+ in the glass structure [4,5]. When increasing the size of the alkali ion, the broad absorption band at about 800 nm in the UV–Vis-NIR spectra is shifted to lower energy (higher wavelengths) [4,6,40,41]. This shift has also been attributed to the difference in the distortion of the octahedron, i.e. when the elongation is not that pronounced, the ligand field strength is decreased, and the absorption band is shifted to a longer wavelength.

According to the crystal field theory (CFT), the difference between the lowest energy levels, the dxy and yz orbitals, and the highest energy level, the dx^2-y^2 orbital, would be higher if the distortion is increased. It means that the difference between the distance of Cu-O_{eq} and Cu-O_{ax} will increase. The results from this investigation show that the distortion of the octahedral geometry is almost the same for all studied glass compositions as can be seen in Tables 2 and 3. The exception for this is the sample named 20 K where the deconvoluted UV–Vis-NIR spectrum looks somewhat different than the others and the calculated distortion is somewhat lower, see Table 3. However, this study also shows that the bond lengths are very similar for all compositions; at least there is no trend in the bond lengths that can explain the decrease in ligand field strength when Na is replaced by K. The term Δ_O is influenced by the type of ligand, the metal ion and the distance from the metal ion to the ligands with the inverse fifth power [42]. This means, if all Cu(II)–O bond lengths in the potassium containing glass would have been longer than the bonds in the glasses with more sodium, that could also (except for being less distorted) have explained the decrease of the ligand field strength as the radii of alkali ion is increased. However, according to the EXAFS measurements, there is no such difference of the Cu(II)–O bond lengths in the octahedral configuration when the glass composition is altered. Thus, there must be another explanation to the observed difference in Δ_O.

In the CFT only ionic bonds are considered. In the ligand field theory (LFT), also the covalent bonding is taken into account. The dz^2 and dx^2-y^2 orbitals of the Cu^{2+} ion and the six O^{2-} ligands form σ-bonds and π-bonds are formed from dxy, dxz and dyz orbitals. As the O^{2-} ions are π-donating ligands they will already have a filled t_{2g} orbital and thus force the metal ion's electrons to the antibonding orbital (t_{2g}^*) which has a higher energy, see Fig. 5. This will lead to a decrease of Δ_O between the t_{2g}^* and e_g^* energy levels compare to when π bonding is neglected. It means that an increase of the covalent character of the Cu(II)–O bond will actually decrease the ligand field strength, Δ_O, compare to the case when the bond has more ionic character. It has been shown that in copper containing potassium aluminosilicate glasses the degree of covalent character (i.e. proportion of π-bonds) for the Cu(II)–O bond is higher than for the Cu(II)–O bond in sodium aluminosilicate glasses [7]. It is possible that the fraction of covalent bonds is higher in the potassium containing glasses in this study, too, thus it would explain the decrease in Δ_O. This explanation was suggested by Lee and Brückner [5] based on EPR and UV–Vis-NIR spectroscopy results from Cu containing alkali silicate glass. However, they concluded that the Jahn-Teller distortion increased with the size of alkali ion.

Both the CFT and the LFT assume the complex-ion to be isolated from the rest of the glassy matrix. It was recently suggested that the surrounding structure (secondary, third, fourth polyhedron… etc.)
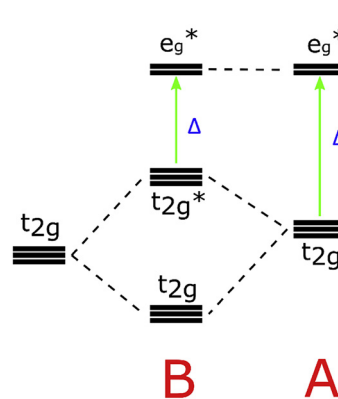

Fig. 5. In A, when π-bonding is ignored and situation B when π-interactions are considered for π-donor ligands.

affects the Δ_O of the distorted Cu^{2+} complex in crystalline samples such as K_2CuF_4 and $KCuF_3$ [43]. Based on ab initio calculations, it was stressed that the potential energy of the neighboring lattices will contribute to the difference in Δ_O. In the present study, the higher field strength of Na^+ compared to K^+ will result in a higher internal electric field (i.e. higher potential energy) which most likely will affect the Cu (II)-oxygen octahedron. This might also explain the differences in ligand field strength in the sodium containing glasses compared to the potassium containing glasses.

The above described picture of how Cu(I) and Cu(II) is incorporated in silicate glass remains quite idealistic; it is likely that copper is not that ordered, as reflected by the large F-factor. However, the very significant 1 s-4p transition which is only seen in linear coordinated Cu(I), is more clearly observed in the samples with higher $[Cu(I)]/[Cu_{tot}]$ ratio (i.e. the Sb containing glasses). Therefore, the conclusion is that Cu(I) is mostly linearly coordinated with two oxygen ions. Concerning the Cu(II) coordination it is noted that the results from an elongated fivefold coordinated square pyramidal coordination look about the same as for the elongated octahedron, in analogy with Cu^{2+} in water [34,39]. The transitions in UV–Vis-NIR would be at the same energies. When this hypothetical coordination was tried during the EXAFS analysis, the obtained fit was almost as good as the one for the elongated octahedron. We mention this because it is important to understand that X-ray and UV–Vis-NIR absorption spectroscopy are methods that delivers data which can be interpreted in more than one way, especially in unorganized materials like glass.

5. Conclusions

EXAFS and XANES investigation showed that Cu(I) in the glass matrix (20-x)Na_2O-xK_2O-10CaO-70SiO_2 is coordinated by two oxygen ions mainly in linear structure, other possible structures gave not as good fits with experimental data. The Cu(I)–O bond lengths were found to be 1.79–1.83 Å (± 0.02 Å). The EXAFS analysis further revealed that the Cu(II) has a coordination of six oxygen ions in an elongated Jahn-Teller distorted octahedral geometry. This structural configuration was confirmed by UV–Vis-NIR spectroscopy. The four equatorial Cu(II)–O bond lengths were found to be 1.89–1.91 Å (± 0.02 Å) and the two axial Cu(II)–O bond lengths were found to be 2.20–2.24 Å (± 0.02). The degree of distortion of the Cu(II)-oxygen octahedron was found to be about the same for all investigated glass compositions. There are other options for Cu(II) to be coordinated when looking at data from EXAFS and UV–Vis-NIR, but not with any support from the literature.

Declaration of Competing Interest

The authors declare that they have no known competing financial interests or personal relationships that could have appeared to

influence the work reported in this paper.

Acknowledgements

References

[1] F. Baucke, J. Duffy, Redox reactions between cations of different polyvalent elements in glass melts: an optical basicity study, Phys. Chem. Glasses 34 (4) (1993) 158–163.

[2] Z.Y. Yao, et al., Structure and mechanical properties of copper-lead and copper-zinc borate glasses, J. Non-Cryst. Solids 435 (2016) 55–68.

[3] B.-S. Bae, M.C. Weinberg, Optical absorption of copper phosphate glasses in the visible spectrum, J. Non-Cryst. Solids 168 (3) (1994) 223–231.

[4] A. Duran, J. Fernandez Navarro, The colouring of glass by Cu^{2+} ions, Phys. Chem. Glasses 26 (4) (1985) 125–131.

[5] J.-H. Lee, R. Brückner, Optische und magnetísche Eigenschaften Cu^{1+}-und Cu^{2+}-haltiger Alkaliborat-,-germanat-und-silicatgläser mit Bezug auf die Borsäuse-und Germanatanomalie, Glastechnische Berichte 57 (2) (1984) 30–43.

[6] L. Grund Bäck, Electronic spectra and molar extinction coefficient of Cu^{2+} in mixed alkali-alkaline earth-silica glasses, Phys. Chem. Glas. - Eur. J. Glass. Sci. Technol. B 56 (1) (2015) 8–14.

[7] A. Klonkowski, Bond character and properties of the mixed alkali system Na_2O-K_2O-Al_2O_3-SiO_2, J. Non-Cryst. Solids 57 (2) (1983) 339–353.

[8] A. Klonkowski, G. Frischat, Properties of mixed alkali glasses in the system Li_2O-Na_2O-Al_2O_3-SiO_2, Phys. Chem. Glasses 24 (2) (1983) 47–53.

[9] S.P. Singh, A. Kumar, Molar extinction coefficients of the cupric ion in silicate glasses, J. Mater. Sci. 30 (11) (1995) 2999–3004.

[10] F. D'Acapito, et al., Local atomic environment of Cu ions in ion-exchanged silicate glass waveguides: an x-ray absorption spectroscopy study, Appl. Phys. Lett. 71 (18) (1997) 2611–2613.

[11] F. D'Acapito, et al., The local atomic order and the valence state of Cu in Cu-implanted soda-lime glasses, J. Non-Cryst. Solids 232 (1998) 364–369.

[12] K. Fukumi, et al., Structural investigation on implanted copper ions in silica glass by XAFS spectroscopy, J. Non-Cryst. Solids 238 (1) (1998) 143–151.

[13] J. Lee, et al., EXAFS study on the local environment of Cu^+ ions in glasses of the Cu_2O–Na_2O–Al_2O_3–SiO_2 system prepared by Cu^+/Na^+ ion exchange, J. Non-Cryst. Solids 277 (2–3) (2000) 155–161.

[14] C. Maurizio, et al., Local coordination geometry around Cu^+ and Cu^{2+} ions in silicate glasses: an X-ray absorption near edge structure investigation, Eur. Phys. B - Condens. Matter Complex Syst. 14 (2) (2000) 211–216.

[15] C. Maurizio, et al., Site of transition metal ions in ion-exchanged metal-doped glasses, Mater. Sci. Eng. B 149 (2) (2008) 171–176.

[16] K. Kamiya, et al., Extended X-ray absorption fine structure (EXAFS) study on the local environment around copper in low thermal expansion copper aluminosilicate glasses, J. Am. Ceram. Soc. 75 (2) (1992) 477–478.

[17] A. Silvestri, et al., The role of copper on colour of palaeo-Christian glass mosaic tesserae: an XAS study, J. Cult. Herit. 13 (2) (2012) 137–144.

[18] T. Bring, et al., Colour development in copper ruby alkali silicate glasses. Part 1. The impact of tin (II) oxide, time and temperature, Glass Technol. 48 (2) (2007) 101.

[19] L. Grund Bäck, Sharafat Ali, S. Karlsson, D. Möncke, E.I. Kamitsos, B. Jonson, Mixed alkali/alkaline earth-silicate glasses: *Physical properties and structure by vibrational spectroscopy*, Int. J. Appl. Glas. Sci. 10 (3) (2019) 349–362.

[20] Peak fit, Systat Software Inc., https://systatsoftware.com/products/peakfit/.

[21] S. Carlson, et al., XAFS experiments at beamline I811, MAX-lab synchrotron source, Sweden, J. Synchrotron Radiat. 13 (5) (2006) 359–364.

[22] G.N. George, I.J. Pickering, EXAFSPAK: A Suite of Computer Programs for Analysis of X-Ray Absorption Spectra, SSRL, Stanford, 1995.

[23] A.L. Ankudinov, J.J. Rehr, Relativistic calculations of spin-dependent x-ray-absorption spectra, Phys. Rev. B 56 (4) (1997) R1712–R1716.

[24] J. Kaufmann, C. Rüssel, Thermodynamics of the Cu^+/Cu^{2+}-redox equilibrium in soda-silicate and soda-lime-silicate melts, J. Non-Cryst. Solids 355 (9) (2009) 531–535.

[25] L. Tröger, et al., Determination of bond lengths, atomic mean-square relative displacements, and local thermal expansion by means of soft-x-ray photoabsorption, Phys. Rev. B 49 (2) (1994) 888–903.

[26] S.I. Andronenko, et al., Local symmetry of Cu^{2+} ions in sodium silicate glasses from data of EPR spectroscopy, Glas. Phys. Chem. 30 (3) (2004) 230–235.

[27] R.P.S. Chakradhar, et al., Mixed alkali effect in borate glasses - electron paramagnetic resonance and optical absorption studies in Cu^{2+} doped xNa_2O–$(30-x)$$K_2O$–$70B_2O_3$ glasses, J. Phys. Condens. Matter 15 (9) (2003) 1469–1486.

[28] J. Kaewkhao, S. Rhianphumikarakit, N. Udomkan, ESR and optical absorption spectra of copper (II) ions in glasses, Adv. Mater. Res. 55-57 (2008) 849–852.

[29] N.S. Rao, et al., Mixed alkali effect in Cu^{2+} doped boroarsenate glasses—EPR and optical absorption studies, Phys. B Condens. Matter 404 (12) (2009) 1785–1789.

[30] T.G.V.M. Rao, et al., Spectroscopical splitting of Cu ion energy levels in magnesium lead fluoro silicate glasses, Phys. B Condens. Matter 407 (4) (2012) 593–597.

[31] A.A. Ahmed, A.F. Abbas, F.A. Moustafa, Mixed alkali effect as exhibited in the spectra of borate glasses containing Cu^{2+}, Phys. Chem. Glasses 24 (2) (1983) 43–46.

[32] T. Kristiansen, et al., Single-site copper by incorporation in ambient pressure dried silica aerogel and xerogel systems: an X-ray absorption spectroscopy study, J. Phys. Chem. C 115 (39) (2011) 19260–19268.

[33] D.M. Pickup, et al., X-ray absorption spectroscopy and high-energy XRD study of the local environment of copper in antibacterial copper-releasing degradable phosphate glasses, J. Non-Cryst. Solids 352 (28) (2006) 3080–3087.

[34] P. Frank, et al., The solution structure of [Cu(aq)]2 + and its implications for rack-induced bonding in blue copper protein active sites, Inorg. Chem. 44 (6) (2005) 1922–1933.

[35] E.I. Solomon, A.B.P. Lever, Inorganic Electronic Structure and Spectroscopy, Applications and Case Studies, vol. 2, Wiley-Interscience, 1999.

[36] B.J. Hathaway, D.E. Billing, The electronic properties and stereochemistry of mononuclear complexes of the copper(II) ion, Coord. Chem. Rev. 5 (2) (1970) 143–207.

[37] R. Shannon, Revised effective ionic radii and systematic studies of interatomic distances in halides and chalcogenides, Acta Crystallogr. Sect. A: Cryst. Phys., Diffr., Theor. Gen. Crystallogr. 32 (5) (1976) 751–767.

[38] B.C. Chakoumakos, J.A. Fernandez-Baca, L.A. Boatner, Refinement of the structures of the layer silicates $MCuSi_4O_{10}$ (M = Ca, Sr, Ba) by Rietveld analysis of neutron powder diffraction data, J. Solid State Chem. 103 (1) (1993) 105–113.

[39] P. Frank, et al., A high-resolution XAS study of aqueous Cu(II) in liquid and frozen solutions: pyramidal, polymorphic, and non-centrosymmetric, J. Chem. Phys. 142 (8) (2015) 084310.

[40] A.A. Ahmed, Effect of Glass Composition on the Stereochemistry of the Cu^{2+} Ion, in International Congress on Glass (ICG), (1983) Hamburg, Germany.

[41] M. Cable, Z.D. Xiang, The optical spectra of copper ions in alkali-lime-silica glasses, Phys. Chem. Glasses 33 (4) (1992) 154–160.

[42] R.G. Burns, Mineralogical Applications of Crystal Field Theory. Mineralogical Applications of Crystal Field Theory, Cambridge University Press, Cambridge, UK, 1993, p. 575.

[43] P. García-Fernández, et al., Compounds containing tetragonal Cu^{2+} complexes: is the $d_{x_2-y_2}$–$d_{3z_2-r_2}$ gap a direct reflection of the distortion? J. Phys. Chem. Lett. 4 (14) (2013) 2385–2390.